

Nonplanar, Noninnocent, and Chiral: A Strongly Saddled Metallocorrole

Abraham B. Alemayehu, Lars Kristian Hansen, and Abhik Ghosh*

Department of Chemistry and Center for Theoretical and Computational Chemistry, University of Tromsø, N-9037 Tromsø, Norway

Received May 10, 2010

The first crystal structure of a copper β -octabromo-*meso*-triarylcorrole exhibits a uniquely saddled corrole macrocycle, where adjacent pyrrole rings are tilted relative to each other by 60–80°. Such strong nonplanarity may be contrasted with the essentially planar macrocycle conformations observed in the vast majority of metalcorrole crystal structures. Density functional theory calculations suggest that two effects, ligand noninnocence and peripheral overcrowding, acting in concert, are responsible for the unique, observed conformation.

Recent findings from our laboratory¹ and elsewhere^{2,3} point to a remarkable aspect of metalcorrole structural chemistry. Group 9 (Co, Rh, Ir) metalcorroles are essentially planar, regardless of steric crowding on the corrole periphery. This has been confirmed, for example, by X-ray crystallographic analyses of cobalt and iridium β -octabromo-*meso*-triarylcorroles.^{2,3} Copper corroles, by contrast, are inherently saddled, even in the absence of steric congestion on the macrocycle periphery.¹ Though somewhat counterintuitive, these generalizations are fully supported by density functional theory (DFT) calculations.¹ Thus, the DFT potential energy curves shown in Figure 1 indicate that the saddling dihedral χ is about 40° even for a sterically unhindered copper triarylcorrole, whereas the corresponding angle is essentially zero for highly sterically hindered cobalt

corroles.¹ Both theoretical considerations and ¹H NMR spectroscopy suggested that the saddling distortions observed for copper corroles are driven by their noninnocent nature,⁴ specifically by a copper($d_{x^2-y^2}$)-corrole(a_{2u}) orbital interaction (shown in Figure 2) that becomes symmetry-allowed as the corrole is saddled.¹ This orbital interaction

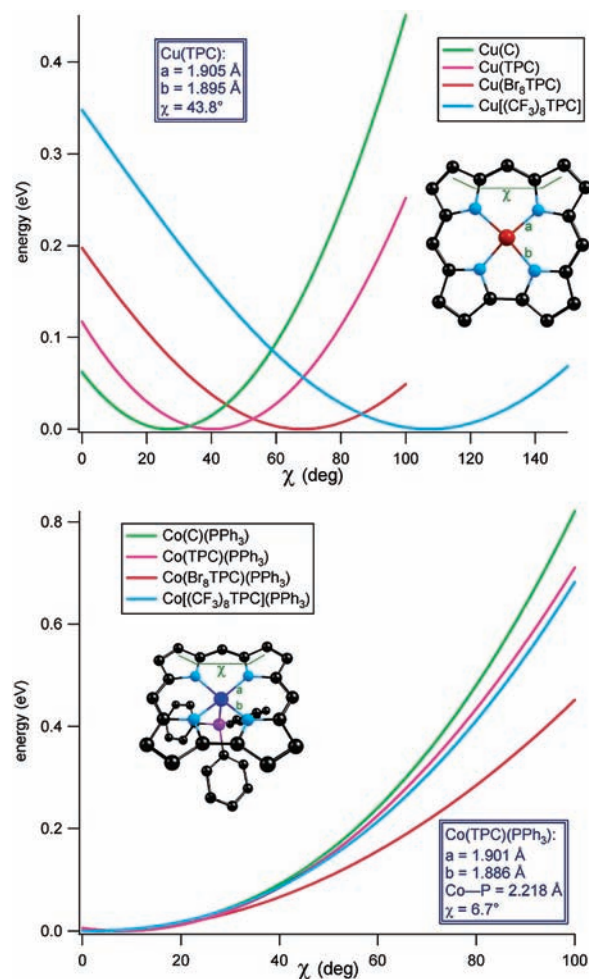


Figure 1. OLYP/STO-TZP saddling potentials for (a) Cu- and (b) Co(PPh₃) corroles as a function of the C₈–C₉–C₁₁–C₁₂ dihedral angle (χ). Geometry parameters for TPC derivatives are shown in the blue insets. Adapted from ref 1.

*To whom correspondence should be addressed. E-mail: abhik.ghosh@uit.no.

(1) Alemayehu, A. B.; Gonzalez, E.; Hansen, L.-K.; Ghosh, A. *Inorg. Chem.* 2009, 48, 7794–7799.

(2) Paolesse, R.; Nardis, S.; Sagone, F.; Khoury, R. G. *J. Org. Chem.* 2001, 66, 550–556.

(3) (a) Palmer, J. H.; Day, M. W.; Wilson, A. D.; Henling, L. M.; Gross, Z.; Gray, H. B. *J. Am. Chem. Soc.* 2008, 130, 7786–7787. (b) Palmer, J. H.; Mahammed, A.; Lancaster, K. M.; Gross, Z.; Gray, H. B. *Inorg. Chem.* 2009, 48, 9308–9315.

(4) Ligand noninnocence is ubiquitous for metalcorroles. For key studies, see: (a) Cai, S.; Walker, F. A.; Licoccia, S. *Inorg. Chem.* 2000, 39, 3466–3478. (b) Ghosh, A.; Wondimagegn, T.; Parusel, A. B. *J. Am. Chem. Soc.* 2000, 122, 5100–5104. (c) Steene, E.; Wondimagegn, T.; Ghosh, A. *J. Phys. Chem. B* 2001, 105, 11406–11413. Addition/correction: *J. Phys. Chem. B* 2002, 106, 5312. (d) Zakhariyeva, O.; Schünemann, V.; Gerdan, M.; Licoccia, S.; Cai, S.; Walker, F. A.; Trautwein, A. X. *J. Am. Chem. Soc.* 2002, 124, 6636–6648. (e) Steene, E.; Dey, A.; Ghosh, A. *J. Am. Chem. Soc.* 2003, 125, 16300–16309. (f) Walker, F. A.; Licoccia, S.; Paolesse, R. *J. Inorg. Biochem.* 2006, 100, 810–837. (g) Roos, B. O.; Veryazov, V.; Conradie, J.; Taylor, P. R.; Ghosh, A. *J. Phys. Chem.* 2008, 112, 14099–14102.

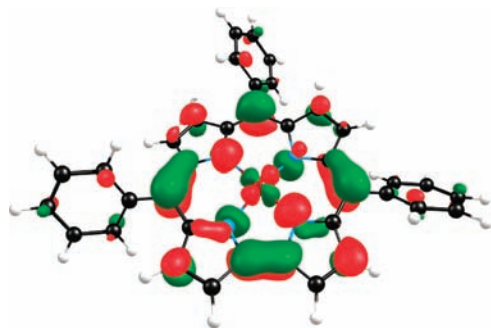


Figure 2. Spin-restricted OLYP/STO-TZP HOMO of Cu(TPC) (contour = $0.05 \text{ e}/\text{\AA}^3$).

allows some of the electron density from the corrole π -HOMO to flow into the otherwise empty Cu $d_{x^2-y^2}$ orbital; thus, copper corrole is not a true copper(III) complex but has significant copper(II) corrole($\bullet 2-$) character. However, evidence for our contention that copper corroles are electronically and stereochemically “special” has remained incomplete in that the very large saddling dihedrals ($\chi \sim 65^\circ$ or higher) predicted in Figure 1 have not been experimentally observed, until now.⁵

Here we report a single-crystal X-ray structure of copper 2,3,7,8,12,13,17,18-octabromo-5,15-bis(4-methoxyphenyl)-10-(4-methylphenyl)corrole, Cu[Br₈-5,15-(4-MeOP)₂-10-(4-MeP)C] (Figure 3). Although the presence of a disordered solvent (*n*-hexane) results in a low proportion of observed reflections, the *R* factor is 4.6% [$I > 2\sigma(I)$] and 6.1% [$I > 1.5\sigma(I)$] and the corrole part of the structure is fully ordered and of high quality. The remarkable feature of the structure, which is the first crystal structure of a Cu[Br₈TPC] derivative, is the strongly saddled nature of the corrole macrocycle. Saddling is unusual for metallocorroles, as noted above specifically with reference to cobalt and iridium corroles,^{2,3} and very strong saddling is unprecedented. The structure reported here, with a χ of 68.2° , is by far the most strongly saddled metallocorrole structure reported to date. Importantly, the experimentally observed saddling dihedral matches perfectly that predicted theoretically for Cu[Br₈TPC] (see Figure 1), providing key support for our theoretical picture of copper

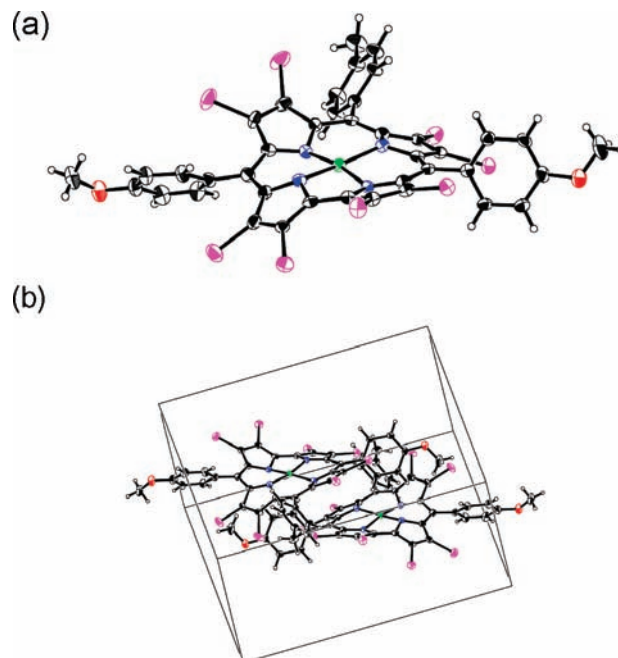


Figure 3. (a) ORTEP for Cu[Br₈-5,15-(4-MeOP)₂-10-(4-MeP)C]. (b) Unit cell.

corroles.¹ By contrast, the cobalt corrole saddling potentials (Figure 1) suggest that corroles are inherently far less prone to saddling than analogous porphyrins. (Recall that there is no precedence for a planar β -octabromo-*meso*-tetraarylmetalloporphyrin.⁶) Against this context, the strong saddling observed here appears to result from two factors acting in concert; initiated by the aforementioned copper corrole orbital interaction,⁷ the saddling is reinforced by steric congestion at the macrocycle periphery.

It is instructive to evaluate the spectroscopic and electrochemical properties of metallocorroles in light of the unique, nonplanar structure reported herein. The strong red shift of the Soret band of the β -Br₈ complex is typical of both β -octahalogenoporphyrins and octahalogenocorroles;⁸ it reflects not only generally smaller π - π^* energy spacings but also kinked intratetrapyrrole dihedral angles attributable to the strongly saddled geometry.^{9,10} However, because of its complex,

(5) For other examples of copper corrole X-ray structures, see: (a) Brückner, C.; Brinas, R. P.; Bauer, J. A. K. *Inorg. Chem.* **2003**, *42*, 4495–4497. (b) Luobeznova, I.; Simkhovich, L.; Goldberg, I.; Gross, Z. *Eur. J. Inorg. Chem.* **2004**, 1724–1732. (c) Bröring, M.; Bregier, F.; Tejero, E. C.; Hell, C.; Hell, C.; Holthausen, M. C. *Angew. Chem., Int. Ed.* **2007**, *46*, 445–448.

(6) For key references to β -octabromo-*meso*-tetraarylporphyrin derivatives, see: (a) Renner, M. W.; Barkigia, K. M.; Zhang, Y.; Medforth, C. J.; Smith, K. M.; Fajer, J. *J. Am. Chem. Soc.* **1994**, *116*, 8582–8592. (b) Ghosh, A.; Halvorsen, I.; Nilsen, H. J.; Steene, E.; Wondimagegn, T.; Lie, R.; van Caemelbecke, E.; Guo, N.; Ou, Z. P.; Kadish, K. M. *J. Phys. Chem. B* **2001**, *105*, 8120–8124. (c) Henling, L. M.; Schaefer, W. P.; Hodge, J. A.; Hughes, M. E.; Gray, H. B.; Lyons, J. E.; Ellis, P. E. *Acta Crystallogr., Sect. E* **1993**, *49*, 1743–1747. (d) Shao, J. L.; Steene, E.; Hoffman, B. M.; Ghosh, A. *Eur. J. Inorg. Chem.* **2005**, 1609–1615.

(7) There is no electronic imperative for a similar orbital interaction in manganese(III), cobalt(III), rhodium(III), and iridium(III) corroles because, unlike copper(III), these are non-high-valent ions. For FeCl corroles, which are high-valent in an overall sense (even though the iron center per se is not high-valent⁴), metal–ligand spin coupling is mediated via an overlap of the d_{z^2} orbital of the intermediate-spin Fe^{III} center and the porphyrin- a_{2u} -like corrole HOMO. When the metal is brought more into the mean plane of the corrole, saddling presumably weakens this coupling. Thus, whereas ordinary FeCl triarylcorroles are $S = 1$, the slightly saddled Fe[Me₈TPC]Cl (Me₈TPC = β -octamethyl-*meso*-triphenylcorrole) is $S = 2$, most likely as a result of ferromagnetic coupling between an $S = 3/2$ Fe^{III} center and a corrole radical: Nardis, S.; Paolesse, R.; Licoccia, S.; Fronczek, F. R.; Vicente, M. G. H.; Shokhireva, T. K.; Cai, S.; Walker, F. A. *Inorg. Chem.* **2005**, *44*, 7030–7046.

(8) For key electronic absorption spectroscopic and spectroelectrochemical studies of copper corroles, see: (a) Wasbotten, I. H.; Wondimagegn, T.; Ghosh, A. *J. Am. Chem. Soc.* **2002**, *124*, 8104–8116. (b) Ou, Z.; Shao, J.; Zhao, H.; Ohkubo, K.; Wasbotten, I. H.; Fukuzumi, S.; Ghosh, A.; Kadish, K. M. *J. Porphyrins Phthalocyanines* **2004**, *8*, 1236–1247. (c) Thomas, K. E.; Wasbotten, I. H.; Ghosh, A. *Inorg. Chem.* **2008**, *47*, 10469–10478.

(9) Although nonplanar porphyrins generally exhibit red-shifted optical spectra, the exact origin of the red shifts is a remarkably subtle issue. DiMaggio and co-workers have shown that the ruffling distortion per se does not lead to red-shifted spectra. Yet, calculations on the actual skeletons of nonplanar porphyrins do show red-shifted spectra. The solution to this conundrum appears to be that distortions along higher-frequency modes (i.e., various kinked dihedrals), as distinct from ruffling per se, lead to the observed red shifts: (a) Wertsching, A. K.; Koch, A. S.; DiMaggio, S. G. *J. Am. Chem. Soc.* **2001**, *123*, 3932–3939. (b) Parusel, A. B. J.; Wondimagegn, T.; Ghosh, A. *J. Am. Chem. Soc.* **2000**, *122*, 6371–6374. (c) Haddad, R. E.; Gazeau, S.; Pécaut, J.; Marchon, J.-C.; Medforth, C. J.; Shelnutz, J. A. *J. Am. Chem. Soc.* **2003**, *125*, 1253–1268. (d) Wasbotten, I. H.; Conradie, J.; Ghosh, A. *J. Phys. Chem. B* **2003**, *107*, 3613–3623.

(10) We have commented elsewhere⁸ on the fact that *meso*-aryl substituents exert far more dramatic effects on the Soret maxima of copper corroles than they do for other metals. This study provides a plausible qualitative explanation of this phenomenon. Copper corroles, because of their potentially strongly saddled geometries, sustain much stronger orbital overlaps between the corrole core and *meso*-aryl groups than do other metallocorroles.

multiorbital character, the red-shifted Soret band does not necessarily indicate a reduced HOMO–LUMO gap. An experimental measure of the latter is provided by $E_{1/2\text{ox}} - E_{1/2\text{red}}$, the so-called “electrochemical HOMO–LUMO gap”. This quantity is higher for the β -Br₈ complex (1.07 V) than for its β -H₈ congener (0.92 V).¹¹ To appreciate the significance of this result, we need to recall that the LUMO of copper corroles is similar in appearance to the HOMO, except that the copper–corrole relative phase is reversed. In other words, the HOMO–LUMO gap may be viewed as a measure of the copper(II) corrole(•2–) antiferromagnetic coupling. Because the strength of this coupling is expected to increase with increasing saddling, it is understandable that the considerably more saddled Cu[Br₈-5,15-(4-MeOP)₂-10-(4-MeP)C] has a higher HOMO–LUMO gap than its β -H₈ analogue.

¹H NMR spectroscopy provided additional support for the above picture of bonding. In contrast with typical β -H₈ copper corroles,^{4c} we found no evidence of *paramagnetic* copper(II) corrole(•2–) excited states (derived from HOMO-to-LUMO excitation) in the ¹H NMR spectrum between –20 and +40 °C. DFT calculations are qualitatively consistent with this observation. Thus, OLYP¹²/TZP calculations¹³ predicted an adiabatic singlet–triplet splitting of 0.6 eV for Cu[Br₈TPC], compared to a value of 0.1 eV for unsubstituted copper corrole.^{4b} Thus, the structural results, electrochemistry, ¹H NMR spectroscopy, and DFT calculations all indicate that β -octabromination results in significantly stronger copper(II)–corrole(•2–) antiferromagnetic coupling. The fact that the different techniques present a mutually consistent picture, while satisfying, is of course only to be expected. What is worth noting is the unique structural consequences of the enhanced spin coupling and the interplay of the

metal–ligand orbital overlap and the steric effects operating at the macrocycle periphery.

A potentially significant footnote to the above story concerns the chirality of copper corroles. As shown in Figure 3, the corrole macrocycle has approximate C₂ symmetry and each unit cell (*P* $\bar{1}$) contains a pair of enantiomeric molecules related by an inversion center. It would be of great interest if the complex studied, or Cu[Br₈TPC] derivatives in general, were resolvable. DFT (OLYP¹²/STO-TZP)¹³ calculations were carried out to determine the energy barrier for saddling-inversion-mediated enantiomerization. For Cu[Br₈TPC], the barrier turned out to be only about 5 kcal/mol (the plausibility of this number may be seen from Figure 1, where the transition state for saddling inversion corresponds to $\chi = 0^\circ$). Resolution of Cu[Br₈TPC] derivatives thus does not appear to be realistic. Even for the considerably more sterically hindered Cu[(CF₃)₈TPC],^{8c} which we have synthesized but not yet crystallographically characterized, DFT calculations predict a saddling-inversion barrier of about 7 kcal/mol. Despite the poor prognosis for straightforward resolution, it may be possible to isolate copper corroles in enantiomerically pure form by complexation with a protein or covalent derivatization with a chiral auxiliary. Once isolated, such derivatives should provide exciting opportunities for fundamental studies of a new inherently chiral chromophore as well as for the elaboration of novel chiral materials.

Acknowledgment. This work was supported by the Research Council of Norway.

Supporting Information Available: Details of synthesis, physical measurements, and X-ray analysis and a CIF file. This material is available free of charge via the Internet at <http://pubs.acs.org>.

(11) Redox potentials (V vs SCE, in CH₂Cl₂ containing 0.1 M TBAP): Cu[5,15-(4-MeOP)₂-10-(4-MeP)C], $E_{1/2\text{ox}} = 0.68$ V, $E_{1/2\text{red}} = -0.24$ V; Cu[Br₈-5,15-(4-MeOP)₂-10-(4-MeP)C], $E_{1/2\text{ox}} = 1.12$ V, $E_{1/2\text{red}} = 0.05$ V.

(12) The OLYP exchange–correlation functional is based on the OPTX exchange functional (Handy, N. C.; Cohen, A. *J. Mol. Phys.* **2001**, *99*, 403–412) and the LYP correlation functional (Lee, C.; Yang, W.; Parr, R. G. *Phys. Rev.* **1988**, *B37*, 785–789).

(13) The calculations were carried out with the ADF program system with methods described in: Velde, G. T.; Bickelhaupt, F. M.; Baerends, E. J.; Guerra, C. F.; Van Gisbergen, S. J. A.; Snijders, J. G.; Ziegler, T. *J. Comput. Chem.* **2001**, *22*, 931–967.